JOURNAL OF GEOPHYSICAL RESEARCH, VOL. 105, NO. B11, PAGES 25,671–25,684, NOVEMBER 10, 2000

Continuous deflation of the Askja caldera, Iceland, during the 1983-1998 noneruptive period

Erik Sturkell and Freysteinn Sigmundsson

Nordic Volcanological Institute, Reykjavík, Iceland

Abstract. The Askja volcano at the spreading plate boundary in north Iceland consists of nested calderas, the latest formed in an eruption in 1875. Several eruptions have occurred since in Askja, the most recent in 1961. Precise leveling has been conducted yearly at Askja since 1983. In 1993, a dense GPS network was measured in and around the Askja caldera consisting of more than 20 points, and we remeasured this complete network for the first time in 1998. Askja subsided during the period from 1983 to 1998. Observed deformation fits broadly with a "Mogi" point source model with best fitting location near the center of the main Askja caldera (65.0448°N, 16.7805°W) at a depth of 2.8 km. From 1983 to 1991 the yearly subsidence rate between the end points of a leveling profile decayed gradually from ~10 mm/yr to an average of ~7 mm/yr in the 1991–1998 period. Total subsidence at the Askja center in the 1983–1998 period is at least 75 cm, and the integrated volume of surface subsidence is ~0.037 km^3. This period has been a "quiet" period at Askja with no eruptions, large earthquakes or known dike injections. Such a high rate of "background" deformation has not been observed at other volcanoes in Iceland. The eruption of a neighboring volcano in 1996 has not resulted in a modified deformation pattern at Askja, indicating no pressure connection at depth between the two systems. Solidification may account for part of the observed contraction and subsidence in Askja.

1. Introduction

The Askja volcano is situated at the divergent (~2 cm/yr) Mid-Atlantic plate boundary in the northern volcanic zone (NVZ) of Iceland (Figure 1). The NVZ north of the Vatnajökull ice cap is composed of five volcanic systems with fissure swarms that are arranged enechelon along the plate boundary, with their long axes slightly oblique to the rift axis. They are from the south to north: Kverkfjöll, Askja, Fremri-Námur, Krafla, and Þeistareykir. The Krafla, Askja, and Kverkfjöll volcanos have developed calderas. Krafla and Askja have had well-documented eruptions after the settlement of Iceland in 874 A.D. Several volcanoes are located south of Askja below Vatnajökull ice cap, including Bárðarbunga and Grímsvötn.

If erupting volcanoes are excluded, the Askja volcano exhibits a much higher rate of ground deformation than has been observed elsewhere in Iceland [*Tryggvason*, 1989a]. Ground deformation studies by leveling were initiated at Askja in 1966, and since 1983 the volcano has been leveled yearly along one leveling profile located in the northeastern part of the main caldera. In 1987 a regional GPS network was installed across the divergent plate boundary in the Askja region with some points close to the volcano. In 1993 a dense GPS network was installed at Askja with a total of 24 sites. We remeasured this network in 1998. In addition, surface tilt has been measured by repeated optical leveling along short arrays of benchmarks. In and around the Askja volcano, 12 such "dry tilt" stations are installed. In this paper, the tilt and leveling data from 1983 to 1998 are presented together with GPS measurements spanning the same 5-year period. These data are then compared to a "Mogi" point source model.

Paper number 2000JB900178
0148-0227/00/2000JB900178$09.00

1.1. Geology and Recent Eruptions

Askja is located within a ~100-km-long and 10 to 15-km-wide fissure swarm (Figure 1). Subaerially erupted basaltic lavas, subaquatic hyaloclastites, and pillow lavas build up the Askja volcanic center, which is in the Dyngjufjöll mountains (Plate 1). It has been active since ~200–300 ka (G. E. Sigvaldason, personal communication, 1999). The volcanic center hosts three calderas. The largest of these is the Askja caldera, formed in the early Holocene, 8 km in diameter [*Sigvaldason*, 1979]. A less pronounced caldera, almost completely filled with lava, is located along the northern edge of the main caldera (Plate 1), and predates it [*Sigvaldason*, 1979]. The youngest nested caldera was formed in a major eruption in 1875 and is today water filled, forming Lake Öskjuvatn. This caldera is 4.5 km in diameter and is ~230 m in depth.

A geothermal area is currently active along the east and south edge of the 1875 caldera, and limited geothermal activity can also be found ~2 km north of the main caldera rim (Plate 1). Pronounced surface geothermal activity is also found in the southeastern part of the Askja caldera, at the Víti crater (phreatic explosion crater from the 1875 eruption), as well as near the eruption sites from 1922 and 1923. The temperature of Lake Öskjuvatn itself is only enhanced in the direct vicinity of the geothermal areas situated along the shore. No geothermal activity occurs today at the most recent eruptive site in Askja, from 1961.

A major rifting event took place in the Askja system in 1874–1876, after more than 400 years of little activity

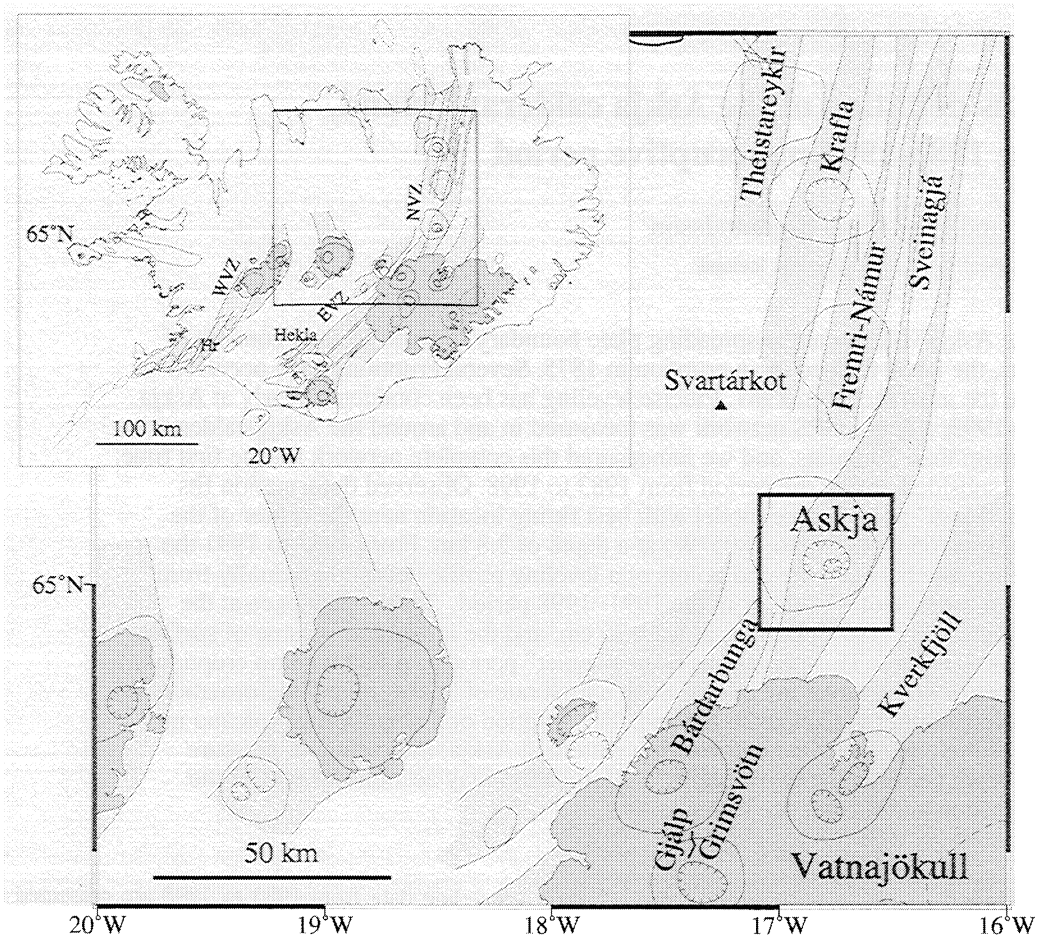

Figure 1. Map of Iceland showing the general outline of the volcanic systems along the plate boundary. The neovolcanic zone in Iceland is divided into the northern volcanic zone (NVZ), the western volcanic zone (WVZ), and the eastern volcanic zone (EVZ). The volcano Hrómundartindur is marked with Hr. Location of the Askja area is outlined by the box. Lightly shaded areas represent fissure swarms connected to central volcanoes (solid lines), and hatch lines mark calderas. Darkly shaded areas represent ice caps. The seismic station Svartárkot of the Icelandic seismic network nearest to Askja is shown by a triangle.

[*Annertz et al.*, 1985; *Brandsdóttir*, 1992]. It included a series of dike injections and basaltic fissure eruptions in the Askja swarm, as well as a large rhyolitic explosive eruption forming the nested Lake Öskjuvatn caldera. The main fissure eruption occurred in the northern part of the Askja fissure swarm (the Sveinagjá graben, ~40 km north of the Askja volcanic center) and generated 0.2–0.3 km^3 of lava there [*Sigvaldason*, 1979]. Shortly after this fissure eruption started, on March 29, 1875, a Plinian eruption occurred and was associated with the formation of the most recent caldera in Askja. This explosive eruption was accompanied by heavy tephra fall to the northeast of Askja, creating 0.21 km^3 dense rock equivalent (DRE) of silicic tephra [*Sparks et al.*, 1981]. It has been suggested [*Sigurdsson and Sparks*, 1978] that magma may have drained laterally from a reservoir beneath the Askja caldera and erupted in the fissure eruption in the Sveinagjá graben. Such lateral drainage of magma might have partly induced the 1875 caldera collapse, which is estimated to have a minimum volume of 1.77 km^3 [*Rist*, 1975; *Sigvaldason*, 1979]. Reports of earthquakes during the 1874–1876 rifting episode indicate that most of the intrusive activity occurred during the first months [*Brandsdóttir*, 1992].

The next eruptive episode at the Askja volcano took place in 1921–1929. During this episode a fissure eruption occurred south of the Dyngjufjöll mountains (Plate 1), as well as several minor eruptions at the 1875 caldera rim. The eruptions near the 1875 caldera rim produced ~0.03 km^{3}of lava, while the fissure eruption generated 0.3 km^3 of lava [*Sigvaldason et al.*, 1992].

The most recent eruption in Askja began on October 26, 1961, and extended into the first days of December of the same year [*Thorarinsson and Sigvaldason*, 1962]. Then an east-west trending fissure opened up close to the rim of the main caldera (Plate 1), and lava flowed out of the caldera through the Öskjuop pass and fanned the plain north of Dyngjufjöll mountains. The volume of the 1961 lava is ~0.09 km^3 [*Sigvaldason et al.*, 1992].

1.2. Seismicity in Askja

During our study period, the permanent Icelandic seismic network only recorded events in the Askja region larger than about *M* 1 (S. Rögnvaldsson, personal communication, 1999). The closest permanent seismometer was located at Svartárkot

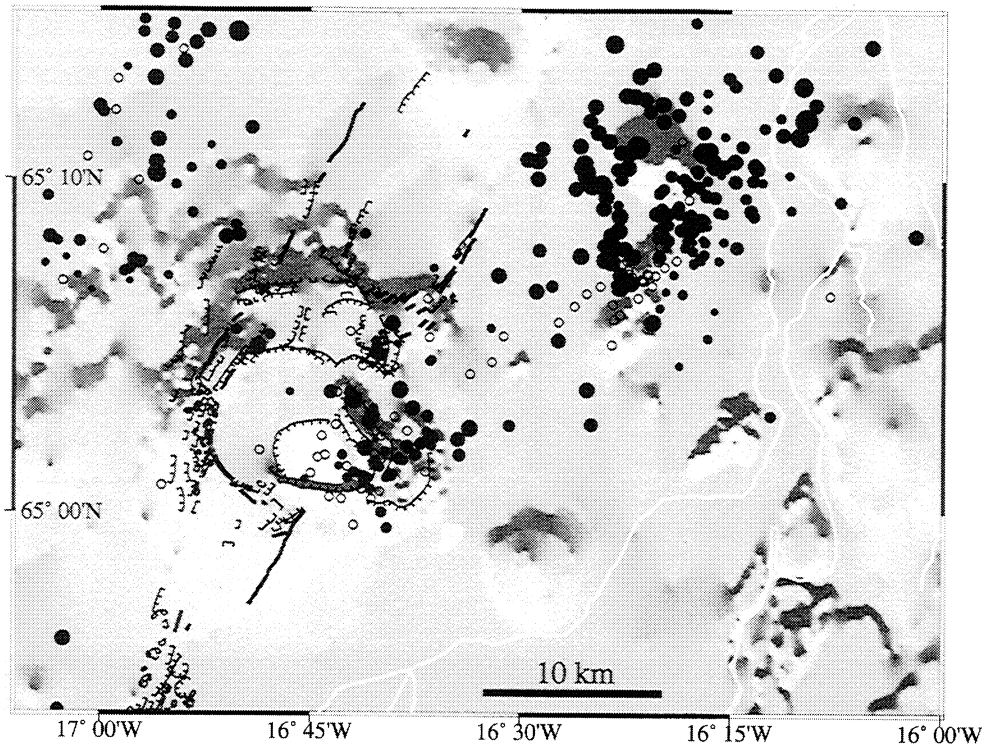

Figure 2. Epicenters of earthquakes in the Askja region, 1973–1998. (Icelandic Meteorological Office, unpublished data, 1973–1998). The size of the solid circles represents the magnitude, which varies from 1 to 4.2. Open circles represent earthquakes with no information of magnitude.

~45 km from Askja (Figure 1). The seismic activity in the Askja region during the 1973 to 1998 is shown in Figure 2 as recorded by the Icelandic seismic network. The location errors are as large as 5 km, but in most cases they are <2 km [*Einarsson and Sæmundsson*, 1987]. The strongest earthquake had a magnitude of 4.2. Most of the earthquakes at Askja volcano proper occur in a cluster beneath the southeastern part of the volcano close to the geothermal areas. *Einarsson* [1991] interpreted these earthquakes as related to geothermal activity. A temporary seismic survey in the summer of 1989 also indicated that the microseismic activity at Askja central volcano is directly related to high-temperature geothermal processes (B. Brandsdóttir, personal communication, 1999). A second cluster is located east of Askja. This cluster formed in two earthquake swarms in the summers of 1982 and 1983 [*Einarsson*, 1991]. A third cluster is northwest of Askja. Neither of the latter two clusters has any surface expression. The earthquake swarms northeast of Askja are not spatially related to any central volcano and lack the persistent nature typical of earthquakes associated with geothermal activity. They are most likely related to plate boundary deformation and slip along regional faults.

2. Deformation Studies

An extensive ground deformation-monitoring network has been installed in the Askja region (Figure 3). It consists of GPS stations, electronic distance measurement (EDM) stations, lake level observations, a leveling profile, and dry tilt stations.

2.1. Leveling and Tilt Measurements

A 1.7-km-long leveling profile was measured yearly from 1966 to 1972 and from 1983 to 1998, but no measurements were conducted in the 1973–1982 period. During 1983 and 1984 the profile was lengthened (Figure 3) but this part of the profile has only been leveled four times. The 1966–1972 measurements showed alternating periods of subsidence and uplift of the caldera floor [*Tryggvason*, 1989a]. Since 1983 the yearly leveling measurements show consistent subsidence toward the central part of the caldera, with yearly relative change in elevation between markers along the profile very similar year after year (Figure 4). It appears that the majority of the deformation is caused by a source under the central part of the main caldera. The profile crosses the 1961 eruptive fissure, and at that location, no discontinuities or change in deformation rate are evident (Figure 4). The source of subsidence is located southwest of the profile, and the closest distance to the source is from benchmarks 406–410 along the profile (Figure 4). The extended part of the leveling profile passes the boundary of the main Askja caldera, covered by 1961 lava. Smooth elevation changes along this part of the profile suggest that no displacement has taken place along a possible caldera boundary fault in this location.

The yearly height difference changes between the reference point (benchmark 404) and the last point along the original profile outward from the caldera center (benchmark 430) indicate some decline in subsidence rate during the 1983–1998 period (Figure 5). This is inferred by subtracting the leveled height difference between benchmarks 404 and

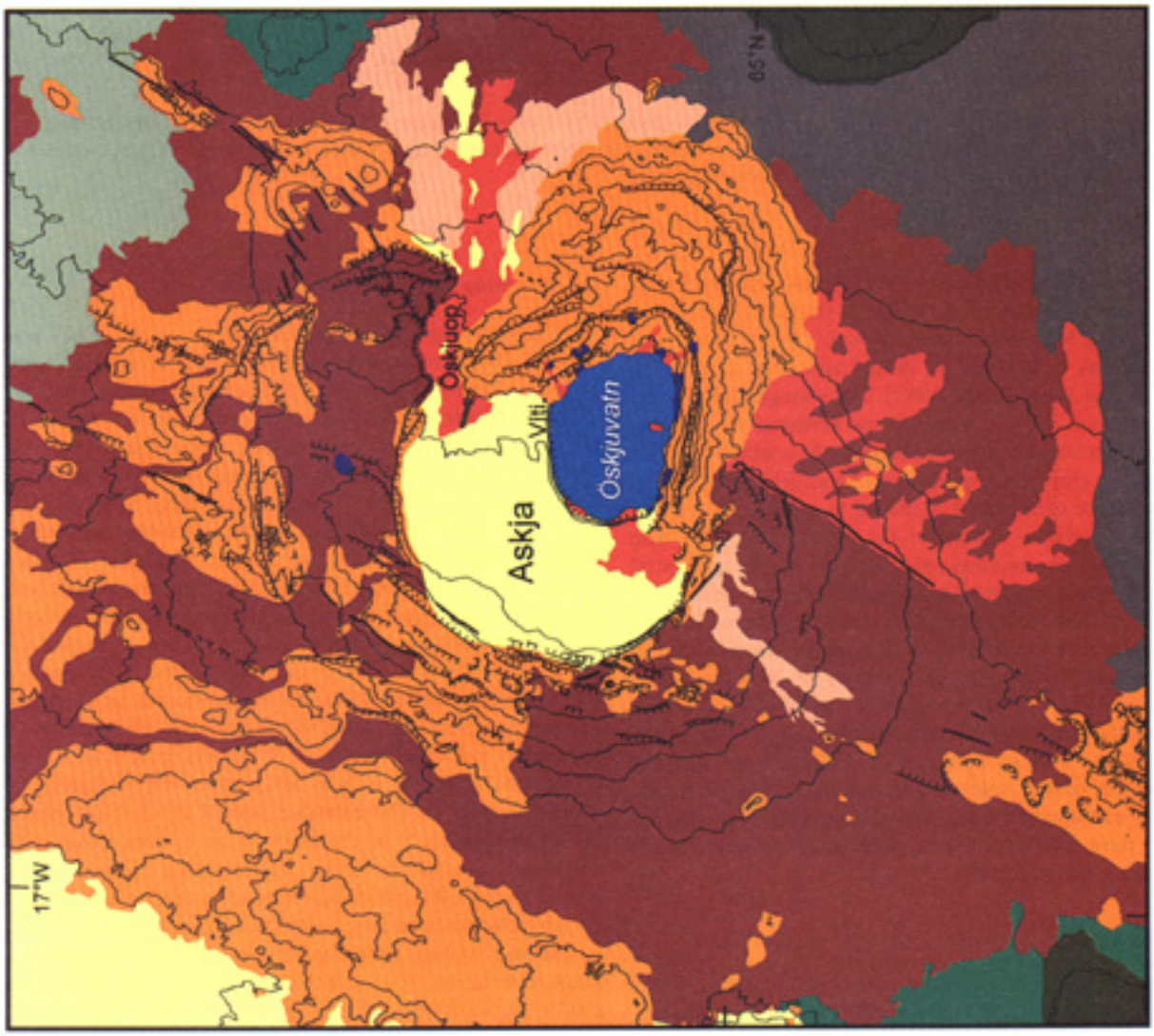

Plate 1. Geological map of the Dyngjufjöll area [modified from *Sigvaldason et al.*, 1992], with the Askja central volcano. The topography is expressed with height contours at 100-m intervals.

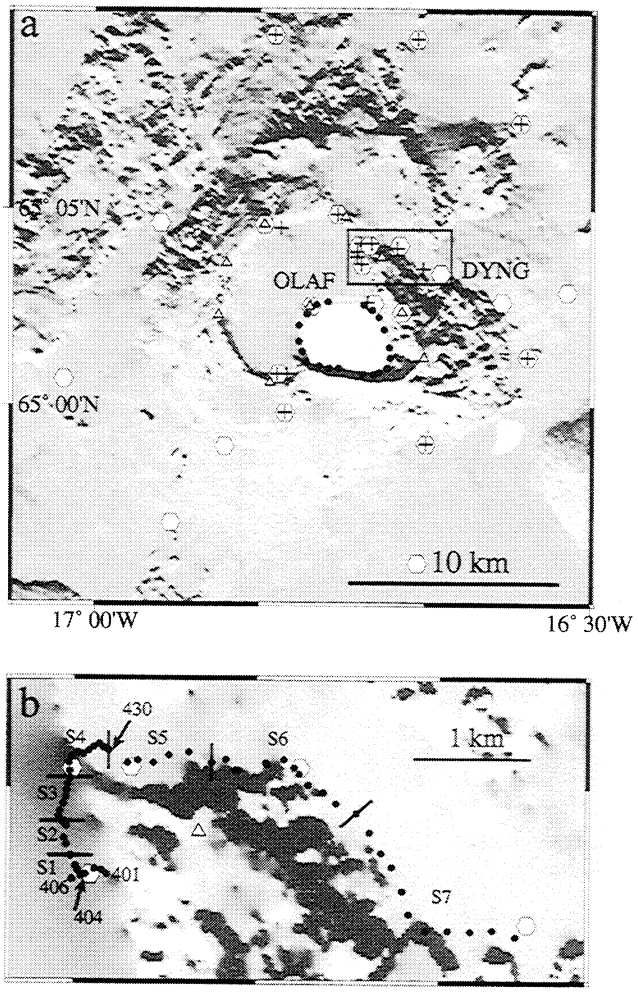

Figure 3. The geodetic network in the Askja region consists of GPS points, and benchmarks for electronic distance measurements (EDM) and optical leveling. (a) The optical leveling is performed along a profile and at tilt stations. Lake level is also measured. The leveled profile is divided into seven sections (S1-S7), and each section is calculated as a tilt station. The S1 to S4 part of the profile has been leveled yearly between 1983 and 1998. The locations of benchmarks 401, 404, 406 and 430 are shown. GPS stations are depicted as hexagons, EDM benchmarks are depicted as triangles, tilt stations are depicted as crosses, and leveling points are depicted as dots. The reference station DYNG was occupied continuously in the 1993 and 1998 GPS surveys. The station OLAF is a GPS and EDM point and a tilt station. (b) Enlargement of the area within the rectangle in (a).

430 for two consecutive years. The relative height difference changes was ~10±0.4 mm/yr for the first 2 years but decayed in the following years, to an average of ~7±0.8 mm/yr since 1991. Point 404 is selected as a reference point (and not a benchmark with a lower number) because it was free of snow every year and could be measured every year [*Tryggvason*, 1989b].

Measurements at dry tilt stations have been conducted at Askja since 1988 [*Rymer and Tryggvason*, 1993]. Initially, two stations were installed, but now there are 12 (Figure 3). Nine of the dry tilt stations in Askja are also GPS stations. We have estimated the average yearly tilt at each of these stations (Figure 6), as the stations have been measured at different times. The tilt vector is the best fitting regression line of all measurements at each station (Figure 6). The number of benchmarks in each station and the distance between them determines the accuracy of the observed tilt. The more benchmarks and the longer the profile, the weaker the tilt signal that can be observed. Using an L-shaped or T-shaped array of 10 bench marks with a distance of 50 m between markers, tilt can be measured with an accuracy of 1 μrad [*Tryggvason*, 1994a]. With stations consisting of benchmarks placed in a circular pattern with a radius of ~25 m, tilt can be measured with an accuracy of 2–5 μrad [*Rymer and Tryggvason*, 1993]. In our analysis of deformation at Askja we followed *Tryggvason* [1989b] and treat segments of the leveling profile as tilt stations. The profile is divided into seven sections S1 to S7 (Figure 3). Sections S1 to S4 have been leveled yearly since 1983 to 1998, while the S5 to S7 part has been leveled four times during this period. Tilt on each of the seven sections of the profile was calculated in the same way as for the tilt station.

2.2. Lake Level Observations

In 1968, 20 benchmarks were installed near the shore all around Lake Öskjuvatn (Figure 3). Repeated measurements of the elevation of these benchmarks above the lake level have then been used to infer relative vertical movements. One benchmark is used as reference, and all the vertical displacement is expressed relative to this point. The estimated observational error was initially ~1–2 cm [*Tryggvason*, 1989a], but after 1985 an improved technique has resulted in somewhat reduced observational errors [*Tryggvason*, 1986]. The lake level has been rising gradually since 1968, inundating several of the benchmarks. Others have been destroyed by rock falls. Of the 20 original benchmarks, only seven were found in 1986 [*Tryggvason*, 1989a]. In 1993, four points were found and leveled, all located on the eastern shore of the lake. The lake level observations alone do not give an acceptable solution to a single point source. However, they indicate that an area northwest of Lake Öskjuvatn near station OLAF (Figure 3) is the location of the subsidence center [*Tryggvason*, 1989a].

2.3. EDM Measurements

In 1982 a network for electronic distance measurements (EDM) was installed in Askja. This network was remeasured and extended in 1985. The network was then remeasured in 1986. The benchmarks are located along the caldera rim, in addition to a central point in the center of the caldera (Figure 3). It is from this central point that all the distances are measured. From 1982 to 1986 all the measured lines contracted, confirming caldera deflation. Measurements conducted in 1993 revealed contraction as well in the 1986–1993 period (E. Tryggvason, unpublished data, 1999).

2.4. GPS Data

The first major GPS campaign in Iceland in 1986 included the installation of a sparse GPS network in the northern volcanic zone of Iceland (NVZ). This network was made denser in 1987. However, the GPS points were still too

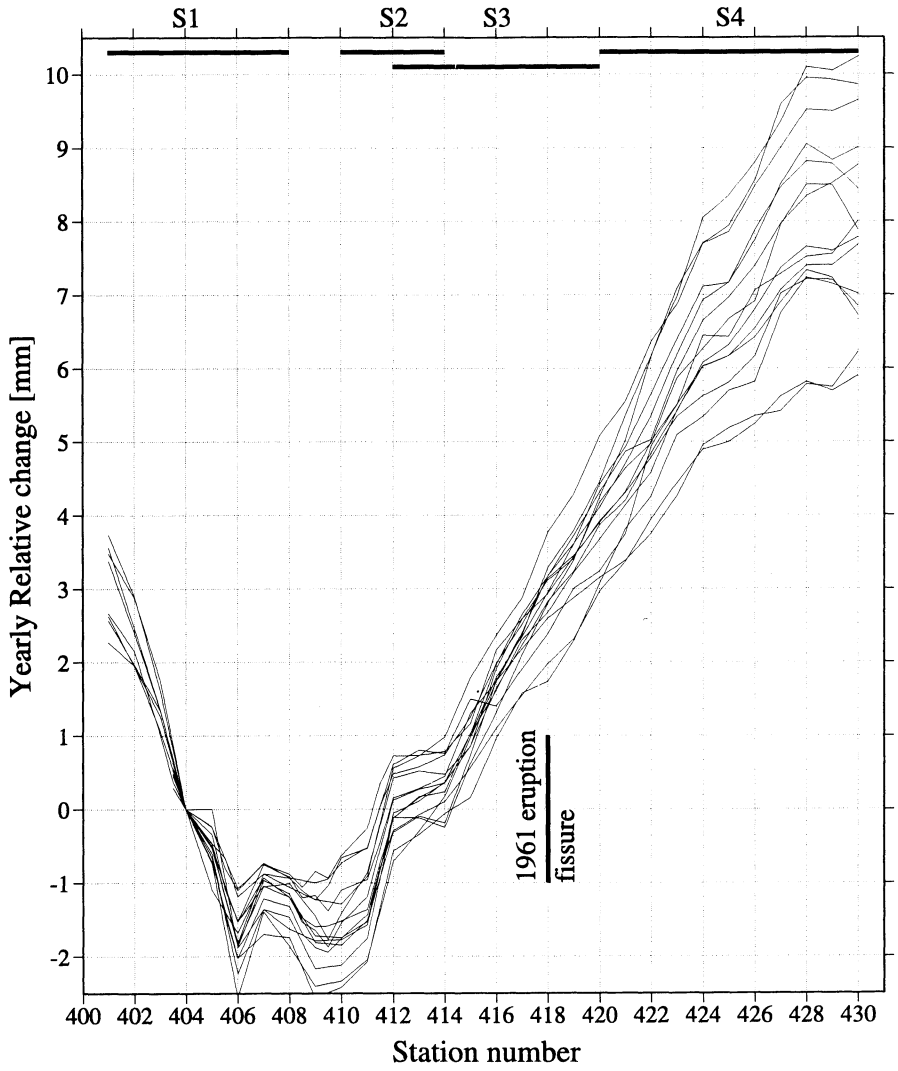

Figure 4. The yearly relative changes along the leveled profile in the period 1983-1998 relative to the benchmark 404. The geometry of the profile is given in Figure 3. Each year a similar pattern is observed and this shows that the rate of subsidence has been approximately constant. The vertical bar shows the location of the 1961 eruptive fissure that strikes near perpendicular to the profile. The bars at the top show the division into sections (S1-S4) that are calculated as tilt stations.

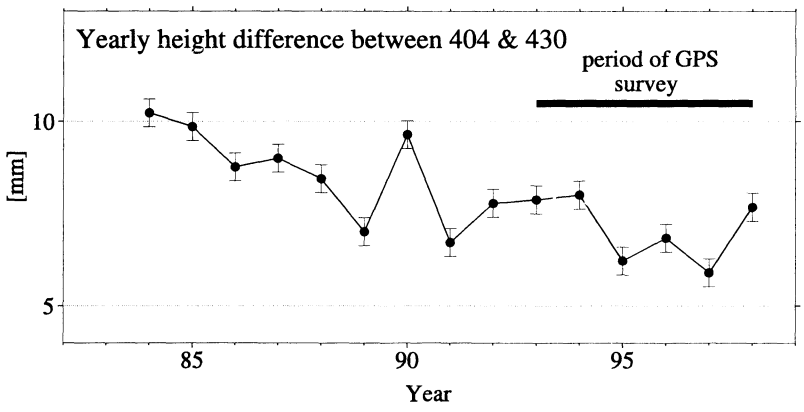

Figure 5. Yearly height differences between the two end points of the leveling profile which have been measured every year, plotted at the end of the time period it covers. Over the period 1983-1998 a slow decay of the rate can be observed, during the time interval of the GPS-measurement, however, the yearly difference has been nearly constant.

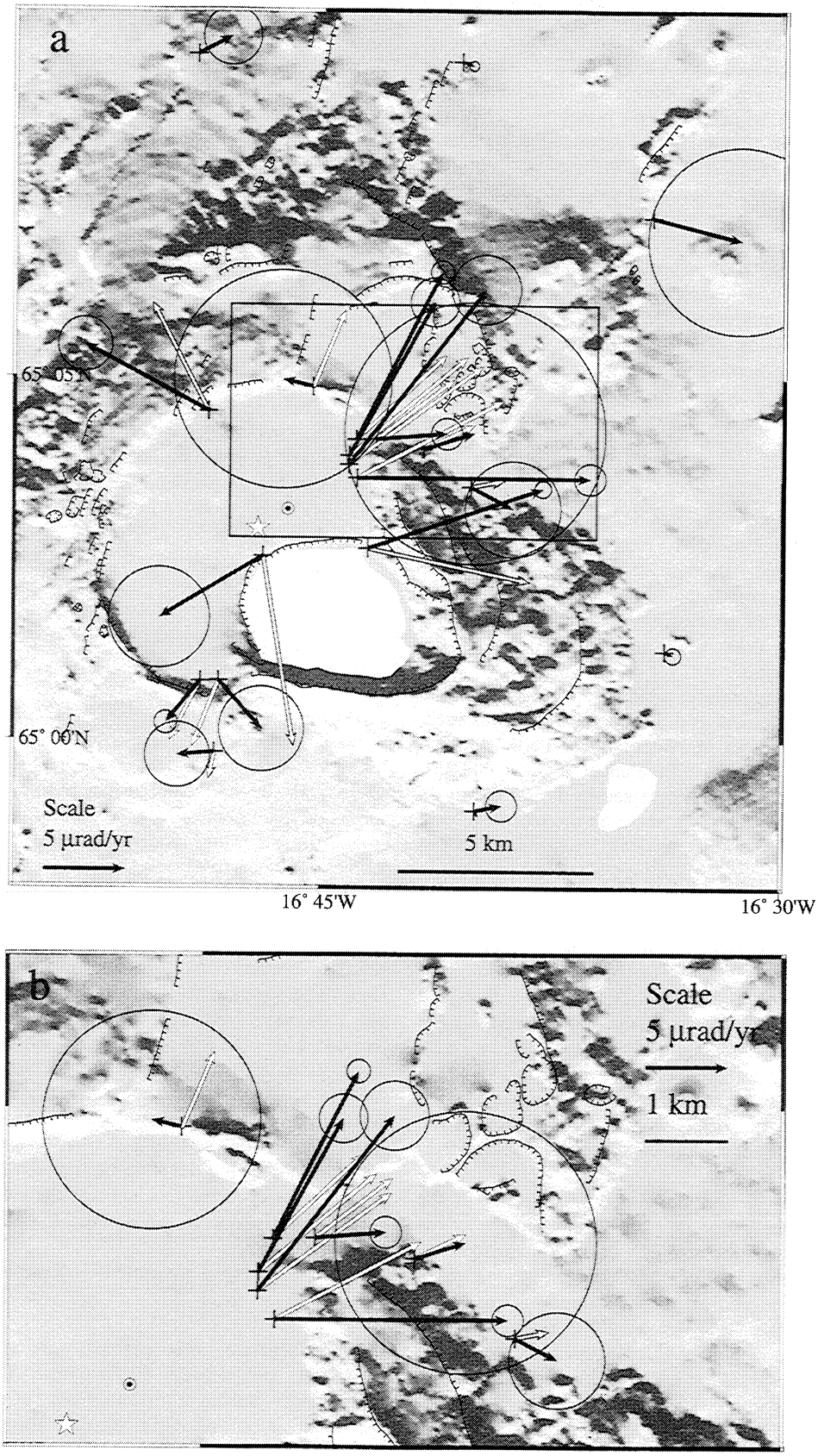

Figure 6. Yearly upward tilt rate at optical leveling tilts stations, 1983-1998 (or shorter) (a) showing the whole area and (b) showing the central part enlarged. Data were extracted from 12 stations and seven sections of the leveling profile, which are calculated as tilt stations. The arrows point away from the center of subsidence. The solid arrows are the measured tilt expressed as tilt per year and the open arrows are best fit model tilt vectors. The size of the tilt exceeds 14 μrad/yr at some stations. The best fitting location (65.0448°N, 16.7805°W) of the combined grid searches is at depth of 2.8 km and is marked by the star. The location of the point source proposed by *Rymer and Tryggvason* [1993] is marked by a circled dot.

sparsely distributed near the Askja volcano for monitoring of its deformation. The first major GPS campaign with a dense network covering Askja was conducted in 1993 [*Camitz et al.*, 1995]. During this survey the number of GPS points was increased to 24 in the Askja region. We remeasured 22 points of this GPS network in 1998 and have generated a 1993-1998 surface displacement solution. During the measurements the DYNG GPS station (Figure 3) served as a reference station and was occupied during the whole of each campaign. The same set of three Trimble 4000 SST GPS receivers were used in the 1993 and the 1998 campaign. Each station was measured for at least three consecutive sessions, each 8 hours long. The observation interval was 15 s.

2.4.1. GPS Processing. The 1993 GPS data was analyzed with version 3.3 of the Bernese GPS software, using broadcast orbits, as discussed by *Camitz et al.* [1995]. In 1998, version 4.0 of the same software was used for processing. For both data sets the reference station DYNG was held fixed in the processing, and the Saastamoinen tropospheric refraction model was used to estimate site tropospheric values.

Of the 21 stations measured in both campaigns, 14 are at a distance of <10 km from the DYNG reference station, and the farthest is 18.7 km away. Because of the limited aperture of the GPS network and short distances between stations, the use of broadcast orbits in the processing of the 1993 data, rather than precise orbits, does not significantly increase the uncertainty of our results.

For the 1998 data, precise orbit information from the Center for Orbit Determination in Europe (CODE), was used, resulting in coordinates in the International Earth Rotation Service (IERS) Terrestrial Reference Frame (ITRF). Otherwise the 1998 data were processed in the same way as the 1993 data. Initially, the raw data from the receivers were transferred into Receiver Independent Exchange (RINEX) format and then into "Bernese" format. The Bernese version 4.0 software [*Rothacher and Mervart*, 1996] was first used to estimate point coordinates, using the ionosphere free linear combination (L3). Next, the software was used to resolve the wide-lane (L5) ambiguities, using the previous L3 coordinate solution as a constraint. The fixed wide-lane ambiguities and the ionosphereic free (L3) linear combination are used to solve for the narrow-lane ambiguities. Subsequently, a final coordinate solution was produced for each measurement session. The result was then combined into one multisession solution by using a statistically correct combination of the single-session solutions of the calculated coordinates and their uncertainties.

Our inferred vertical and horizontal movements in the 1993–1998 period are given in Plate 2 and Figure 7. The vertical movements are presented as a contour map (Plate 2), relative to the reference station DYNG, which is set to zero. The contouring of the vertical displacement was conducted using functions in the GMT software [*Smith and Wessel*, 1990]. Initially, horizontal displacements were inferred relative to the reference station DYNG. Our best fitting Mogi model (described in section 3) suggests, however, that station DYNG was displaced horizontally 3.71 cm in azimuth 263.9°, during the 1993–1998 period. This displacement vector was added to all stations, resulting in the pattern displayed in Figure 7.

3. Modeling

The observed surface deformation of Askja during 1983–1998 resembles that caused by a point source of decreasing pressure. We have chosen the simplest available model, the Mogi model [*Mogi*, 1958], to fit our observations (Figure 8). Elasticity theory is used to calculate the deformation caused by a point source of pressure [*Mogi*, 1958]. The model has three parameters for location (latitude, longitude, and depth) and one parameter that relates to the strength of the source. The strength parameter C is

$$C = \frac{3a^3 \Delta P}{4\mu} = h_0 d^2, \tag{1}$$

where ΔP is the change in fluid pressure within a small sphere with radius a and μ denotes the rigidity of the surrounding crust. The strength parameter can also be related to vertical displacement h_0 at the surface directly above the point source ($r = 0$) and the source depth d. Surface deformation is given by

$$u_r = \frac{h_0 d^2 r}{(d^2 + r^2)^{3/2}}, \tag{2}$$

$$u_z = \frac{h_0 d^3}{(d^2 + r^2)^{3/2}}, \tag{3}$$

$$\delta = \frac{-3h_0 d^3 r}{(d^2 + r^2)^{5/2}}, \tag{4}$$

where r is the horizontal distance from the source, u_r is horizontal displacement, u_z is vertical displacement, and δ is ground tilt. The Mogi model is valid for finite size spherical sources as long as $(a/d)^5 << 1$ [*McTigue*, 1987].

We used forward modeling to fit our observations, utilizing a grid over latitude, longitude, and depth for different values of h_0. Initially, a coarse search was done to infer the permissible limits of h_0. This gave a range of 0.04 – 0.06 m/yr. Then three separate grid searches, with h_0 set to 0.04, 0.05, and 0.06 m/yr were conducted to find the point location (latitude, longitude and depth) of the source that best fits the observations at Askja. The difference between the predicted and the observed observation (displacement components or tilt) at each measured point gives a residual value. In each grid search (horizontal, vertical and tilt) we used a least squares criterion minimizing the χ^2 merit function [*Bevington*, 1969]. The ratio between the residual and the estimated one sigma uncertainty σ is squared and summed to give a χ^2 value:

$$\chi^2 = \sum \left(\frac{\text{predicted} - \text{observed}}{\sigma} \right)^2. \tag{5}$$

Three separate grid searches were performed for tilt, horizontal, and vertical displacement. These suggested a source depth ranging from 2 to 4 km but agreed well on the horizontal location. Grid search using the horizontal displacements gave the lowest χ^2 values at a shallow depth, but the same horizontal location in all grid searches. The minimum χ^2 value in the grid search using horizontal data was

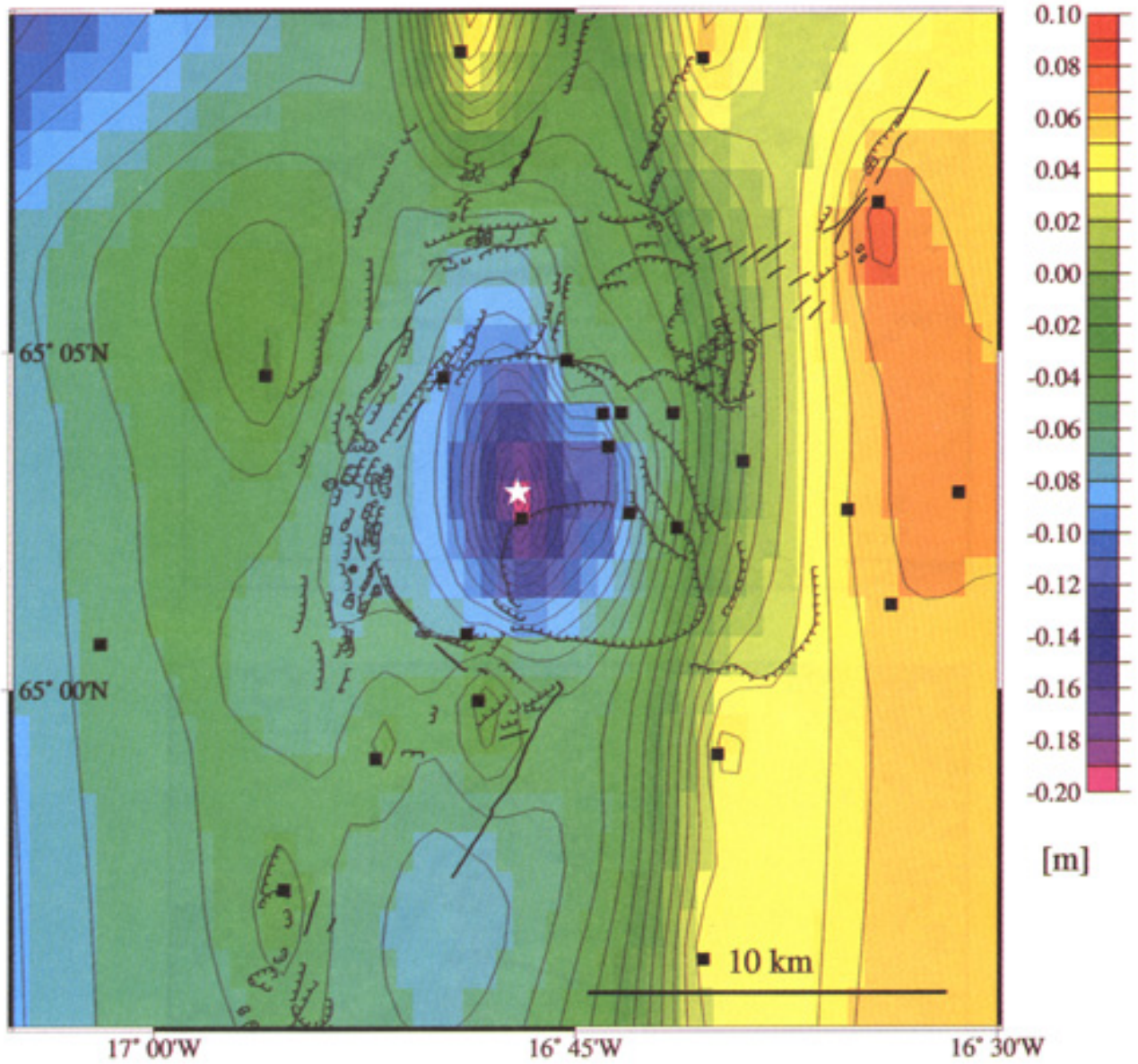

Plate 2. Contour map of vertical displacements during the time period 1993-1998. The contour interval is 2 cm. The maximum relative subsidence is 25 cm. The GPS stations are shown as solid squares. The map shows two features, a circular subsidence in the center of the caldera and an east-west gradient. The uncertainty of the vertical displacement varies between ±0.8 and ±1.5 cm. Star denotes best fit point source location.

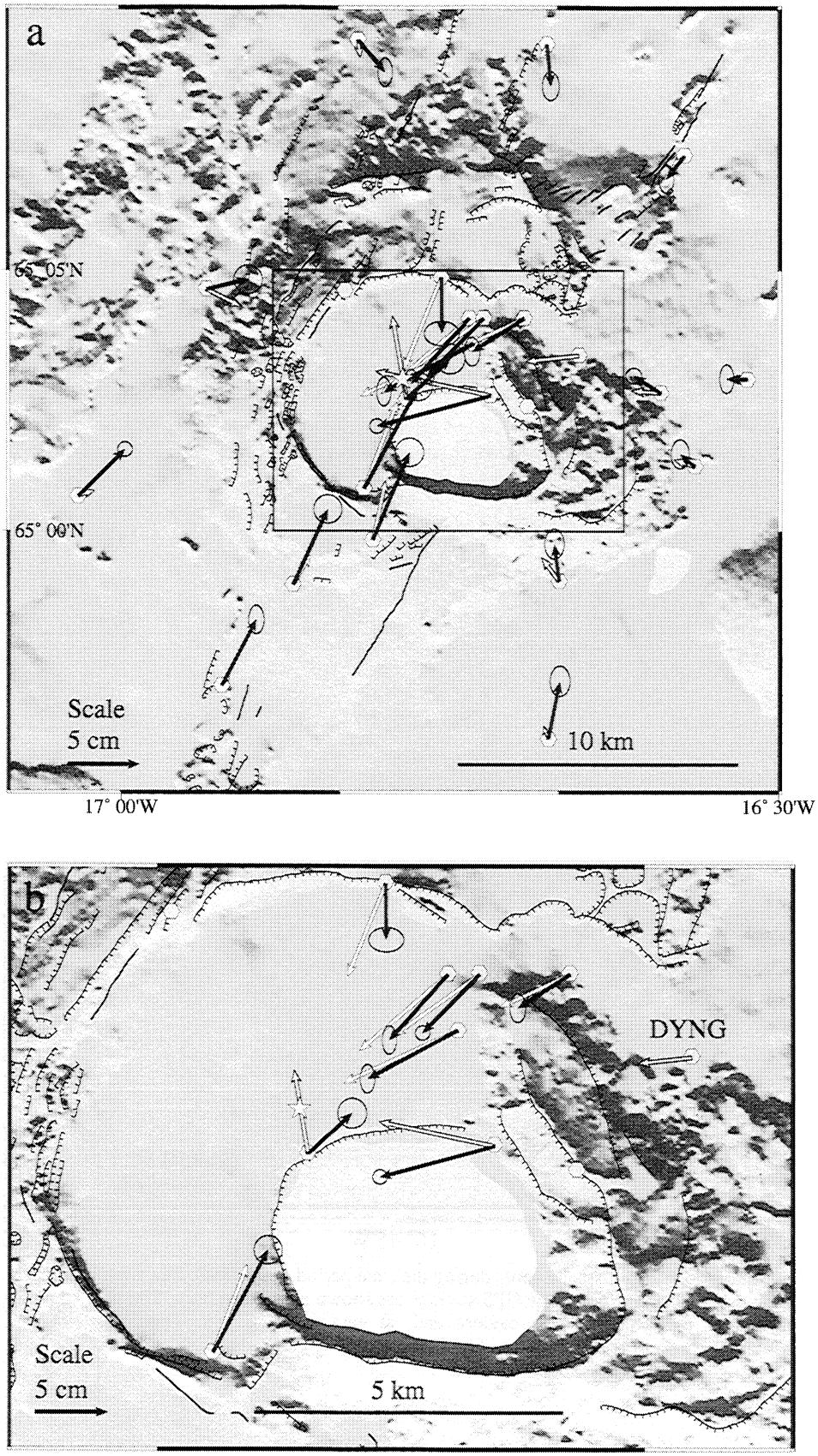

Figure 7. Observed horizontal displacements for the time period 1993-1998 and calculated displacement for the best fitting model. Most of the vectors point toward the caldera, indicating contraction. (a) The whole area. (b) The central part enlarged. The solid arrows are the measured horizontal displacements, and the open arrows are the vectors for the best fit model for the horizontal displacement. The best fitting Mogi source gave an estimate for the displacement of the reference station DYNG (open arrow), resulting in this pattern of vectors. The estimated movement of the DYNG station is 3.71 cm at 263.9°. Star denotes best fit point source location.

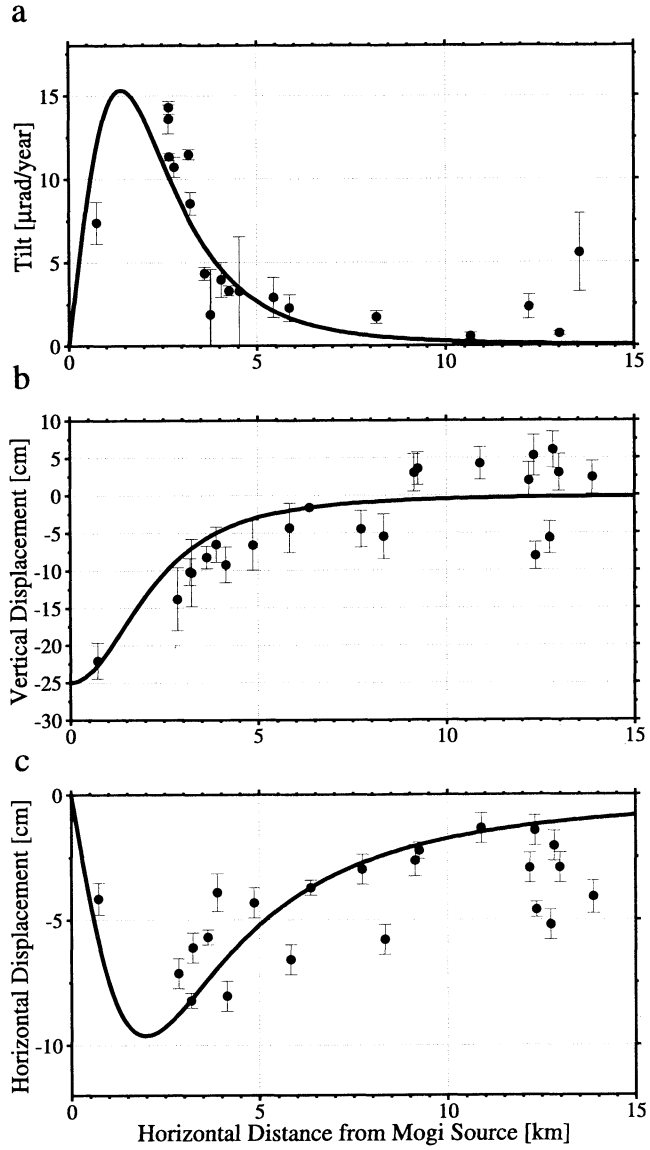

Figure 8. Best fitting Mogi model for (a) the observed yearly tilt, (b) observed vertical and (c) horizontal displacements (between 1993 and 1998) plotted versus the distance from the Mogi source. The tilt is expressed as a yearly rate with the model parameters h_0 = 0.05 m and depth of 2.8 km. The vertical and horizontal displacements cover a 5-year period and have the model parameters set to h_0 = 0.25 m and depth of 2.8 km. Error bars on observations represent 95% confidence limits.

61. The grid search based on the vertical data resulted in horizontal location in good agreement with the search using the horizontal displacements, and its depth was constrained to be <4 km. However, the lowest value χ^2 = 529 for the grid search based on the vertical data suggests a deeper point source and places the center away from majority of the observation points, southwest of the caldera center. Subsidence of the stations to the west of Askja and uplift of the stations east of Askja probably heavily influence this search. A grid search based on the tilt data gave a χ^2 minimum at about the same horizontal location as the other grid searches, with a depth of the pressure source at 2.8 km. For the tilt grid search the χ^2 minimum value was 238. The horizontal grid search resulted in the lowest χ^2 value, indicating that the horizontal movements are better fitted than the vertical and tilt data. However, in our final solution we decided to give equal weight to each type of observation (horizontal displacement, vertical displacement, tilt). This was implemented by scaling the χ^2 values from each type of observation by their respective minimum value and then summing them. Our best fitting point source location is the one that minimized this combined sum. The best fitting location is at (65.0448°N, 16.7805°W), at a depth of 2.8 km. It is marked with a star in Plate 2 and in Figures 6 and 7.

The amount of subsidence is the best-constrained variable in our estimation. The smallest misfit was found with a h_0 value of 0.05±0.005 m/yr. This h_0 value is well constrained by the measurements since the closest station OLAF (Figure 3) is located horizontally only ~0.7 km from the suggested center of subsidence. The direct GPS-measurements yielded subsidence of this station of 0.204±0.008 m relative to the reference station for the 5-year period. The reference station DYNG (Plate 2) is located within the deformation field caused by the subsidence in the center of the main caldera, and its estimated subsidence is 0.016 m in the same period.

The best fitting Mogi source gave an estimate for the vertical and horizontal displacement of the reference station. For each location in the grid search the amount of displacement at the reference station caused by the Mogi source was calculated. All the stations were then corrected for this displacement, and thereafter the χ^2 sum was calculated for the best fitting point source. The vertical displacement for the reference station is -0.0163 m, and this is added to all stations. The same procedure was applied to infer the horizontal displacements (Figure 7). The displacement vector at the reference station inferred from the best fitting Mogi model that is 3.71 cm at 263.9° (open arrow in Figure 7).

4. Discussion

Our inferred location of a pressure source at Askja agrees with the results of *Tryggvason* [1989a] to within 1 km in horizontal position, and is at the same depth. The continuous surface subsidence of Askja for the time period 1983–1998 generates an integrated surface deflation volume of 0.037 km^3. This volume is given by $\Delta V_e = 2\pi h_0 d^2$, with a total subsidence of 0.75 m and a depth of 2.8 km (assuming a Poisson's ratio of 0.25). The corresponding subsurface volume change of the Mogi source is two thirds of the integrated surface deflation volume, or ~0.025 km^3. If this volume change is due to solidification of magma, or outflow of magma from a chamber, then it represents a minimum estimate of magma that has moved or solidified, as bulk expansion of remaining magma in a magma chamber can affect such estimates [*Johnson et al.*, 2000].

Askja is located at the divergent plate boundary in the NVZ of Iceland, and there the full plate spreading rate, according to the NUVEL-1A plate motion model [*DeMets et al.*, 1994], is 1.81 cm/yr. Regional GPS measurements during the 1987–1990 period [*Heki et al.*, 1993] show, however, widening of 2.4 cm/year across at least a 30-km-wide plate boundary deformation zone within which Askja is situated. Our measured GPS network in Askja stretches 24 km in an east-west direction and is within the plate boundary deformation zone. Our horizontal displacements indicate only contraction toward the caldera. The network is not wide enough to observe the plate movements (Figure 7). The residual horizontal deformation field does not show a component of

east-west expansion across Askja, suggesting that the plate boundary zone is much wider than our 24-km-wide GPS network.

Although the vertical deformation at Askja is dominated by a subcircular subsidence in the central part of the Holocene caldera, a second component in the vertical deformation field is evident. This is a regional component, manifested as subsidence on the west side of Askja relative to its east side (Plate 2). The area west of Askja is in the northern continuation of the Bárðarbunga volcanic system (Figure 1). This subsidence might be related to the Gjálp subglacial fissure eruption that took place in 1996 under Vatnajökull. No horizontal widening is, however, seen in the area. Removing the overall westward gradient in the regional vertical deformation field gives a somewhat better fit to the Mogi model for the vertical displacement, while incorporating a plate boundary induced horizontal extension does not considerably improve the fit to the Mogi model. The regional component was not removed in the final model because the GPS survey does not extensively cover the area west of Askja and the few data points do not fully constrain the vertical regional deformation field in this region. The effect of the regional vertical component causes the distant points west of Askja to lie under the model curve and the distant points to the east to lie above it (Plate 2 and Figure 8b). The signal generated by the subsidence dominates greatly over the regional component.

The rate of ground deformation is much higher in Askja than observed at any other dormant volcano in Iceland. Askja hosts the most recent caldera formed in Iceland, the nested 1875 caldera. The most recent eruption in the Askja volcano was in 1961 when a fissure opened along the caldera boundary fault (Plate 1) extruding a volume of 0.09-0.1 km^3 of lava. During the monitored period (1983–1998) one major eruption in a neighboring volcanic system occurred in 1996, when a 7-km-long eruptive fissure opened between the Bárðarbunga and Grímsvötn volcanoes, the Gjálp eruption [*Gudmundsson et al.*, 1997] (see Figure 1).

To gain further understanding of the ongoing deformation at Askja, we compare it to the behavior of some other well-monitored volcanoes in Iceland, including Krafla, Hekla and Hrómundartindur (Figure 1). Hekla and Hrómundartindur volcanoes have deeper deformation sources than at Askja. Deformation at Hekla has been modeled by a point source ranging in depth from 5 to 9 km [*Kjartansson and Gronvold*, 1983; *Tryggvason*, 1994a; *Sigmundsson et al.*, 1992; *Linde et al.*, 1993]. It is interpreted as a deep magma chamber, and there are indications of rapid inflow of magma into it immediately after an eruption. Geodetic measurements show that the Hrómundartindur volcano inflated at a rate ~2 cm/yr during the 1992–1998 period [*Sigmundsson et al.*, 1997a; *Feigl et al.*, 2000]. The geodetic data are consistent with a 6.5±3 km deep pressure source, explained by magma accumulation [*Sigmundsson et al.*, 1997a].

The well-monitored Krafla volcano is more similar to Askja. It has a 3-km-deep magma chamber [*Brandsdóttir et al.*, 1997; *Tryggvason*, 1994b; *Sigmundsson et al.*, 1997b] and a caldera that formed about ~100 ka. An extensive geodetic network was built up at Krafla during a rifting episode that occurred from 1975 to 1984. During that rifting episode the shallow magma chamber inflated due to inflow of magma from below. This was interrupted ~20 times by sudden deflation events accompanying eruptions and/or dike injections. The total horizontal extension in the Krafla rift segment during the episode was ~9 m [*Tryggvason*, 1994b]. The shallow magma reservoir continued to expand for about 5-years after the last eruption in 1975–1984 rifting episode [*Tryggvason*, 1994b]. This pattern changed in 1989 when gradual subsidence began, at a rate of ~5 cm/yr in the 1989–1992 period [*Tryggvason*, 1994b]. *Sigmundsson et al.* [1997b] used satellite radar interferometry to detect a declining subsidence rate in Krafla. They showed that the subsidence rate is much less in the 1993–1995 period, than in the 1992–1993 period. *Sigmundsson et al.* [1997b] interpreted the main cause of the subsidence to be cooling, contraction, and ductile flow of material away from the spreading axis. The deformation in Krafla can be attributed to postrifting relaxation of stress in the crust after the 1975–1984 rifting episode. Decay with time of the rate of crustal deformation is then expected. The caldera floor of Askja has on the other hand subsided during the whole of the 1983–1998 period, as the yearly height changes along the leveled profile indicate (Figures 4 and 5). Those height changes show a higher subsidence rate in the first years than during the time period between the GPS campaigns in 1993 and 1998. The maximum subsidence is in the center of the caldera, ~0.7 km from the GPS station OLAF (Figure 3). At the center the yearly subsidence rate was ~5±0.3 cm/yr in the 1993–1998 period. Measurements in the summer of 1999 indicate that this pattern was continuous.

The yearly leveling performed by Tryggvason showed alternating periods of subsidence and uplift of the caldera floor during the 1966 and 1972 period. The inflation between 1970–1972 was rapid, possibly as much as 20 cm/yr [*Tryggvason*, 1989a]. This rapid uplift was related to renewed inflow of magma and put a definitive end to a possible relaxation of Askja after the 1961 eruption.

The location of Askja on the divergent plate boundary may explain some of the observed subsidence, as its magmatic system is subject to continual extension. However, the same amount of subsidence is not evident at other volcanoes on the plate boundary in Iceland. Pressure oscillation of the Iceland mantle plume could also be a factor. Low pressure in the Icelandic mantle plume could result in decreased pressure at Askja and cause deflation [*Tryggvason*, 1989a]. Pressure connection between neighboring volcanic systems has also been suggested [*Einarsson*, 1987]. However, the eruption of a neighboring volcano in 1996 did not result in a modified deformation pattern at Askja. This indicates that no pressure pulse has moved between the two systems. During the 1996 subglacial Gjálp eruption a 6-7 km long and 200-300 m high hyaloclastite ridge was formed with a volume of 0.7-0.75 km^3 (~0.4 km^3 DRE) [*Gudmundsson et al.*, 1997]. This eruption did not affect the deformation field in Askja.

Magma drainage into the Askja fissure swarm may accommodate some of subsidence. However, no rapid changes in the subsidence rate have been detected since 1983 and no seismic tremors or earthquake swarms suggestive of dike injections have been recorded. No new ground fractures have been observed in the area.

Rymer and Tryggvason [1993] performed a combined study of temporal variations of gravity and elevations changes in Askja during the period 1988-1991. They argue that a point source at 2.5-3.0 km beneath the caldera center (circled dot on Figure 6 at 65.05312°N, 16.76833°W) can account for most of the observed deformation during that period. According to

their study, there is an indication that 80% of the deformation can be accounted for without subsurface mass changes. Solidification and cooling of magma give a volume contraction of about 10% [e.g., *Sigmundsson et al.*, 1997b]. Thus, to cause a deflation volume of 0.025 km^3, solidification of ~0.25 km^3 magma is needed.

5. Conclusion

The crustal deformation data used in this study result from yearly leveling along a profile since 1983, dry tilt measurements and two GPS-campaigns (1993 and 1998) in the region. These data show that the Askja volcano has been subsiding for at least 15 years, with a total amount of subsidence of at least 0.75 m. No slip has been observed along the caldera boundary fault during the study period. The deformation of the leveled profile indicates a continuous subsidence with a center in the main caldera (Figure 4). The subsidence of the caldera floor in Askja takes place without large earthquakes, but during the study period the permanent seismic network of Iceland was not capable of recording earthquakes less than magnitude 1 in Askja. Little or no brittle deformation has occurred during this period, and elastic movements have taken up the majority of the deformation. Most of the deformation can be accounted for by a point source of pressure decrease (a Mogi model) near the center of the main Askja caldera at a depth of 2.8 km.

Deformation attributable to plate spreading is not evident in our 24-km-wide GPS-network covering Askja. The subsidence rate in Askja shows small decay with time (Figure 5), smaller than observed at the Krafla volcano [*Sigmundsson et al.*, 1997b]. In Krafla the subsidence was interpreted as a result of contraction as the magma solidified. We suggest that magma solidification is an important process to explain the long-term subsidence in Askja but regional deformation and slow drainage of magma into the rift zone may contribute to some extent. The exact cause of the deformation still remains uncertain.

Acknowledgments. The authors would like to express their gratitude to Eysteinn Tryggvason and Halldór Ólafsson for all their work in Askja making this paper possible. Without the significant help by Sigrún Hreinsdóttir the GPS processing would have been much more difficult. We thank Sigurður Th. Rögnvaldsson for providing earthquake information before he tragically died in an accident in 1999. We like to thank all the many people that have participated in the collection of geodetic data at Askja and Guðmundur E. Sigvaldason, Bryndís Brandsdóttir, and Thóra Árnadóttir for fruitful discussions and information. We are also grateful for the help of Rósa Ólafsdóttir and Guðmundur H. Guðfinnsson. All except one figure were made with the public domain GMT software.

Reference

Annertz, K., M. Nilsson, and G. E. Sigvaldason, The postglacial history of Dyngjufjöll, *Rep. 8503*, Nord. Volcanol. Inst., Univ. of Iceland, Reykjavík, 1985.

Bevington, P. R., *Data Reduction and Error Analysis*, McGraw-Hill, New York, 1969.

Brandsdóttir, B., Historical accounts of earthquakes associated with eruptive activity in the Askja volcanic system, *Jökull, 42*, 1-12, 1992.

Brandsdóttir, B., W. Menke, P. Einarsson, R. S. White, and R. K. Staples, Færoe-Iceland ridge experiment 2. Crustal structure of the Krafla central volcano, *J. Geophys. Res., 102*, 7867-7886, 1997.

Camitz, J., F. Sigmundsson, G. Foulger, C. -H. Jahn, C. Völksen, and P. Einarsson, Plate boundary deformation and continuing deflation of the Askja volcano, north Iceland, determined with GPS, 1987-1993, *Bull. Volcanol., 57*, 136-145, 1995.

DeMets, C., R. G. Gordon, D. F. Argus, and S. Stein, Effect of recent revision to the geomagnetic reversal time scale on estimates of current plate motions, *Geophys. Res. Lett., 21*, 2191-2194, 1994.

Einarsson, P., The anomalous mantle beneath Iceland and possible pressure connection between volcanoes, paper presented at Symposium on How Volcanoes Work, Hilo, January 19-25, 1987.

Einarsson, P., Earthquakes and present-day tectonism in Iceland, *Tectonophysics, 189*, 261-279, 1991.

Einarsson, P., and K. Sæmundsson, Earthquake epicenters 1982–1985 and volcanic systems in Iceland, map in: Í hlutarins eðli: Festschrift for Thorbjörn Sigurgerirsson, edited by Sigfússon, T. Menningarsjóður, Reykjavík, 1987.

Feigl, K. L, J. Gasperi, F. Sigmundsson, and A. Rigo, Crustal deformation near Hengill volcano, Iceland 1993-1998: coupling between magmatism and faulting inferred from elastic modeling of satellite radar interferograms, *J. Geophys. Res., 105*, in press, 2000.

Gudmundsson, M. T., F. Sigmundsson, and H. Björnsson, Ice-volcano interaction of the 1996 Gjálp subglacial eruption, Vatnajökull, Iceland. *Nature, 389*, 954-957, 1997.

Heki, K., G. R. Foulger, B. R. Julian, and C. -H. Jahn, Plate dynamics near divergent boundaries: Geophysical implications of postrifting crustal deformation in NE Iceland, *J. Geophys. Res., 98*, 14279-14297, 1993.

Johnson, D. J., F. Sigmundsson, and P. T. Delaney, Comment on "Volume of magma accumulation or withdrawal estimated from surface uplift or subsidence, with application to the 1960 collapse of Kīlauea volcano" by P.T. Delaney and D.F. McTigue, *Bull. Volcanol., 61*, 491-493, 2000.

Kjartansson, E., and K. Gronvold, Location of a magma reservoir beneath Hekla volcano, Iceland, *Nature, 301*, 139-141, 1983.

Linde, A. T., K. Agustsson, I. S. Sacks, and R. Stefansson, Mechanism of the 1991 eruption of Hekla from continuous borehole strain monitoring, *Nature, 365*, 737-740, 1993.

McTigue, D. F., Elastic stress and deformation near a finite spherical magma body: Resolution of the point source paradox, *J. Geophys. Res., 92*, 12,931-12,940, 1987.

Mogi, K., Relations between the eruptions of various volcanoes and the deformation of the gound surface around them, *Bull. Earthquake Res. Inst. Univ. Tokyo, 36*, 99-134, 1958.

Rist, S., Stöduvötn, in Icelandic, *Rep. OS-Vatn 7503*, Nal. Energy. Auth., Reykjavík, Iceland, 1975.

Rothacher, M., and L. Mervart, Bernese GPS software version 4.0. Astron. Inst., Univ. of Bern, Bern, Switzerland, 1996.

Rymer, H., and E. Tryggvasson, Gravity and elevation changes at Askja, Iceland, *Bull. Volcanol., 55*, 362-371, 1993.

Sigmundsson, F., P. Einarsson, and R. Bilham, Magma chamber deflation recorded by the Global Positioning System: The Hekla 1991 eruption, *Geophys. Res. Lett., 19*, 1483-1486, 1992.

Sigmundsson, F., P. Einarsson, S. Th. Rögnvaldsson, G. R. Foulger, K. M. Hodgkinson, and G. Thorbergsson, The 1994-1995 seismicity and deformation at the Hengill triple junction, Iceland: Triggering of earthquakes by minor magma injection in a zone of horizontal shear stress, *J. Geophys. Res., 102*, 15,151-15,161, 1997a.

Sigmundsson, F., H. Vadon, and D. Massonnet, Readjustment of the Krafla spreading segment to crustal rifting measured by satellite radar interferometry, *Geophys. Res. Lett., 24*, 1843-1846, 1997b.

Sigurdsson, H., and R. S. J. Sparks, Rifting episode in north Iceland in 1874-1875 and the eruption of Askja and Sveinagja, *Bull. Volcanol., 41*, 149-167, 1978.

Sigvaldason, G. E. Rifting, magmatic activity and interaction between acid and basic liquids. The 1875 Askja eruption in Iceland, *Rep. 7903*, Nord. Volcanol. Inst., Univ. of Iceland, Reykjavík, 1979.

Sigvaldason, G. E., K. Annertz, and M. Nilsson, Effect of glacier loading/deloading on volcanism: postglacial volcanic production rate of the Dyngjufjöll area, central Iceland, *Bull. Volcanol., 54*, 385-392, 1992.

Smith, W. H. F., and P. Wessel, Gridding with continuous curvature splines in tension, *Geophysics*, 55, 293-305, 1990.

Sparks, R. S. J., L. Wilson, and H. Sigurdsson, The pyroclastic deposits of the 1875 eruption of Askja, Iceland. *Philos. Trans. R. Soc. London, 299*, 241-273, 1981.

Thorarinsson, S., and G. E. Sigvaldason, The eruption in Askja, 1961 a preliminary report, *Am. J. Sci., 260*, 641-651, 1962.

Tryggvason, E., Myvatn lake level observations 1984–1986 and ground deformation during a Krafla eruption, *J. Volcanol. Geotherm. Res., 31*, 131-138, 1986.

Tryggvason, E., Ground deformation in Askja, Iceland: Its source and possible relation to flow of the mantle plume, *J. Volcanol. Geotherm. Res., 39*, 61-71, 1989a.

Tryggvason, E., Measurement of ground deformation in Askja 1966 to 1989, *Rep. 8904*, Nord. Volcanol. Inst., Univ. of Iceland, Reykjavík, 1989b.

Tryggvason, E., Observed ground deformation at Hekla, Iceland prior to and during the eruptions of 1970, 1980-1981 and 1991, *J. Volcanol. Geotherm. Res., 61*, 281-291, 1994a.

Tryggvason, E., Surface deformation at the Krafla volcano, north Iceland, 1982-1992, *Bull. Volcanol., 56*, 98-107, 1994b.

E. Sturkell and F. Sigmundsson, Nordic Volcanological Institute, Grensásvegur 50, IS-108 Reykjavik, Iceland. (e-mail: erik@norvol.hi.is and fs@norvol.hi.is).

(Received September 2, 1999; revised April 17, 2000;
accepted May 16, 2000.)